

Transient $A + B \rightarrow 0$ Reaction on Fractals: Stochastic and Deterministic Aspects

G. Zumofen,¹ J. Klafter,² and A. Blumen³

In this paper we study the transient diffusion-limited $A + B \rightarrow 0$, $A_0 = B_0$ annihilation via deterministic reaction-diffusion equations and via simulation of the stochastic many-particle problem. We show that the two approaches are not equivalent and that the deterministic expressions capture only part of the picture. A lower bound is derived for the density decay which indicates that the overall density follows the power law $t^{-\alpha}$ with $\alpha = \min(\tilde{d}/4, 1)$. Hierarchical oscillations superimposed on the power-law decay are observed for reactions on Sierpinski gaskets.

KEY WORDS: $A + B \rightarrow 0$; fractals.

Diffusion-limited bimolecular reactions $A + B \rightarrow \text{inert}$ on regular and fractal structures are of much interest. The time evolution of the particle densities, segregation phenomena, and the dependence on the dimensionality of the problem have been studied in detail.⁽¹⁻¹²⁾ In former works we analyzed the problem through stochastic simulation calculations.^(5,6) An analytical description is possible if one starts from the coupled diffusion-reaction equations which for Euclidean lattices have the form^(1,2,10-14)

$$\begin{aligned}\dot{A}(\mathbf{x}, t) &= D \nabla^2 A(\mathbf{x}, t) - \kappa A(\mathbf{x}, t) B(\mathbf{x}, t) \\ \dot{B}(\mathbf{x}, t) &= D \nabla^2 B(\mathbf{x}, t) - \kappa A(\mathbf{x}, t) B(\mathbf{x}, t)\end{aligned}\tag{1}$$

where $A(\mathbf{x}, t)$ and $B(\mathbf{x}, t)$ are the spatial particle density distributions, D is the diffusion coefficient, and κ denotes the bimolecular reaction rate. Equa-

This work is dedicated to Prof. George H. Weiss.

¹ Laboratorium für Physikalische Chemie, ETH-Zentrum, CH-8092 Zürich, Switzerland.

² School of Chemistry, Tel-Aviv University, Tel-Aviv, 69978 Israel.

³ Physics Institute and BIMF, University of Bayreuth, W-8580 Bayreuth, Germany.

tions (1) are far from being exact, since they are restricted to first-order density functions. Consequently, the reaction term $-\kappa A(\mathbf{x}, t) B(\mathbf{x}, t)$ is only approximate since—at least—the joint probability density of A–B pairs is needed for a correct description.⁽¹¹⁾ In this study we consider an equal number of A and B particles: $A_0 = B_0$, which implies $A(t) = B(t)$ at all times. The analysis of Eq. (1) is simplified by setting $q(\mathbf{x}, t) = A(\mathbf{x}, t) - B(\mathbf{x}, t)$ and $s(\mathbf{x}, t) = A(\mathbf{x}, t) + B(\mathbf{x}, t)$, which leads to

$$\dot{q}(\mathbf{x}, t) = D \nabla^2 q(\mathbf{x}, t) \quad (2)$$

$$\dot{s}(\mathbf{x}, t) = D \nabla^2 s(\mathbf{x}, t) - (\kappa/2)[s^2(\mathbf{x}, t) - q^2(\mathbf{x}, t)] \quad (3)$$

We point out that Eq. (2) holds exactly irrespective of the approximation introduced in expressions (1) for the description of the reaction term.⁽¹¹⁾ The time evolution of the densities is obtained from the spatial or ensemble average: $A(t) = \langle A(\mathbf{x}, t) \rangle_{\mathbf{x}} = 1/2 \langle s(\mathbf{x}, t) \rangle_{\mathbf{x}}$.

In this paper we proceed as follows: We first rewrite the deterministic approach, Eqs. (1)–(3), for discrete lattices so that the equations hold generally also for fractals. From the density difference function we derive an expression for a lower bound for the density decay which holds generally both for regular and for fractal structures. We solve the deterministic equations numerically for Euclidean lattices and Sierpinski gaskets and compare the results with those obtained from simulations of the stochastic problem. Our findings show that the overall decay is well represented by $t^{-\alpha}$, $\alpha = \min(\tilde{d}/4, 1)$, where \tilde{d} is the spectral dimension for fractals and d for regular lattices. The application of this decay law for fractals has been recently a matter of debate.^(4,5,9,15,16)

For discrete lattices Eqs. (2) and (3) are given without loss of generality as a system of coupled differential–difference equations:

$$\dot{q}(\mathbf{x}_j, t) = \Gamma \sum_{i \in \sigma_j} [q(\mathbf{x}_i, t) - q(\mathbf{x}_j, t)] \quad (4)$$

$$\dot{s}(\mathbf{x}_j, t) = \Gamma \sum_{i \in \sigma_j} [s(\mathbf{x}_i, t) - s(\mathbf{x}_j, t)] - (\kappa/2)[s^2(\mathbf{x}_j, t) - q^2(\mathbf{x}_j, t)] \quad (5)$$

where \mathbf{x}_j are the sites, σ_j denotes the nearest neighbors of site j , and Γ is the hopping rate between nearest-neighbor sites. Equations (4) and (5) hold for fractals as well as for Euclidean lattices; they offer a means to avoid the problem of how to generalize the Laplacian to fractals. The solution of Eq. (4) can be written in terms of the Green's function $P(\mathbf{x}_j, t; \mathbf{x}_0, 0)$, the conditional probability to be at \mathbf{x}_j at time t having started at \mathbf{x}_0 at time zero. One has

$$q(\mathbf{x}_j, t) = \sum_i P(\mathbf{x}_j, t; \mathbf{x}_i, 0) q(\mathbf{x}_i, 0) \quad (6)$$

where $q(\mathbf{x}, 0)$ denotes the initial random configuration. $\langle q(\mathbf{x}, t) \rangle_{\mathbf{x}}$ is zero at all times and the second moment averaged over space and over initial configurations is

$$\langle q^2(t) \rangle = \langle q^2(\mathbf{x}, t) \rangle_{\mathbf{x}} = N^{-1} \sum_j \left\langle \left[\sum_i P(\mathbf{x}_j, t; \mathbf{x}_i, 0) q(\mathbf{x}_i, 0) \right]^2 \right\rangle_{\text{init. config.}} \quad (7)$$

Here N denotes the number of lattice sites considered in the model. As initial distributions we take ($q_0/2$ being the initial occupation probability for A or B particles)

$$q(\mathbf{x}_j, 0) = \begin{cases} +1 & \text{with probability } q_0/2 \\ -1 & \text{with probability } q_0/2 \\ 0 & \text{with probability } 1 - q_0 \end{cases} \quad (8)$$

Inserting Eq. (8) into Eq. (7), the configurational average is straightforward, since the $P(\mathbf{x}_j, t; \mathbf{x}_i, 0)$ are independent of the initial configuration:

$$\begin{aligned} \langle q^2(t) \rangle &= N^{-1} \sum_{j,i,k} P(\mathbf{x}_j, t; \mathbf{x}_i, 0) P(\mathbf{x}_j, t; \mathbf{x}_k, 0) \langle q(\mathbf{x}_i, 0) q(\mathbf{x}_k, 0) \rangle_{\text{init. config.}} \\ &= q_0 N^{-1} \sum_{j,i,k} P(\mathbf{x}_j, t; \mathbf{x}_i, 0) P(\mathbf{x}_j, t; \mathbf{x}_k, 0) \delta_{ik} \\ &= q_0 N^{-1} \sum_{j,i} P^2(\mathbf{x}_j, t; \mathbf{x}_i, 0) \end{aligned} \quad (9)$$

To proceed, we consider the Chapman–Kolmogorov equation:

$$P(\mathbf{x}_j, t; \mathbf{x}_i, 0) = \sum_m P(\mathbf{x}_j, t; \mathbf{x}_m, t') P(\mathbf{x}_m, t'; \mathbf{x}_i, 0), \quad 0 \leq t' \leq t \quad (10)$$

which applies for all Markovian processes (irrespective of lattice structure and dimension, i.e., also for fractals). Furthermore, for the system given by Eqs. (4) and (5), the propagator is symmetrical (*vide infra*):

$$P(\mathbf{x}_j, t; \mathbf{x}_i, 0) = P(\mathbf{x}_i, t; \mathbf{x}_j, 0) \quad (11)$$

By inserting Eqs. (10) and (11) into Eq. (9), we find that

$$\begin{aligned} \langle q^2(t) \rangle &= q_0 N^{-1} \sum_j P(\mathbf{x}_j, 2t; \mathbf{x}_j, 0) \\ &= q_0 P(0, 2t) \end{aligned} \quad (12)$$

where $P(0, t)$ is the probability to be at the origin after time t , averaged over all starting sites. Equation (12) relates $\langle q^2(t) \rangle$ to the well-understood

autocorrelation function $P(0, t)$, whose leading behavior follows asymptotically⁽⁷⁾ the power law: $P(0, t) \sim a_{\bar{d}} t^{-\bar{d}/2}$. The prefactor $a_{\bar{d}}$ depends on the details of the lattice.

We note that the symmetry of the propagator, Eq. (11), is fundamental for the derivation of Eq. (12). The symmetry is obvious for ordered lattices. For disordered lattices, Eqs. (4) and (5) correspond in the discrete picture to the “blind-ant” model: all rates between neighboring sites are equal, so that particles stay longer on sites with low coordination number z . The time needed to go along any path from \mathbf{x}_i to \mathbf{x}_j (including stops) is identical to that needed for the reverse path. To test this conclusion, we have focused on percolation clusters. We determined the propagator by solving the master equation:

$$\dot{P}(\mathbf{x}_j, t; \mathbf{x}_0, t_0) = \Gamma \sum_{i \in \sigma_j} [P(\mathbf{x}_i, t; \mathbf{x}_0, t_0) - P(\mathbf{x}_j, t; \mathbf{x}_0, t_0)] \quad (13)$$

where σ_j denotes the nearest neighbors of site j on the cluster. As initial condition we took

$$P(\mathbf{x}_j, 0; \mathbf{x}_0, 0) = \delta_{\mathbf{x}_j, \mathbf{x}_0} \quad (14)$$

Our numerical results support the conclusion that for propagators on percolation clusters, as defined in Eqs. (13) and (14), the symmetry relation (11) holds.

We continue by discussing the implications of Eq. (12) for the density decay. From Eq. (6) one can view q at long times as being a large sum of terms ± 1 or zero, weighted with the corresponding P factors; thus, for large t the central-limit theorem applies, so that $q(\mathbf{x}, t)$ becomes Gaussian-distributed.^(2,13) Therefore

$$q(t) \equiv \langle |q(\mathbf{x}, t)| \rangle_{\mathbf{x}} = [(2/\pi) \langle q^2(t) \rangle]^{1/2}$$

holds in general. If one can now approximate $s(t) = \langle s(\mathbf{x}, t) \rangle_{\mathbf{x}}$ through $q(t)$, then by using Eq. (12) it follows that

$$A(t) = \langle A(\mathbf{x}, t) \rangle_{\mathbf{x}} = 1/2s(t) \gtrsim 1/2q(t) = [q_0 P(0, 2t)/2\pi]^{1/2} \quad (15)$$

which, considering the power-law description for $P(0, t)$, leads to

$$A(t) \gtrsim C_{\bar{d}} A_0^{1/2} t^{-\bar{d}/4} \quad (16)$$

with the constant being $C_d = \pi^{-1/2}(\tau/4\pi)^{d/4}$ for Euclidean lattices and $C_{\bar{d}} = (a_{\bar{d}}/\pi)^{1/2} (\tau/2)^{\bar{d}/4}$ for Sierpinski gaskets. Here, τ is the hopping time, which for structures where the sites have a unique coordination number z

is $\tau^{-1} = z\Gamma$. For hypercubic lattices, setting $D = (2\tau)^{-1}$, C_d is identical to the results of ref. 2. Thus expressions (15) and (16) derived for the general case including fractals reproduce exactly the results of Euclidean lattices.⁽²⁾

The point is now whether setting $q(t) \simeq s(t)$ is permitted.^(1,2,11-13) To settle the question, one has to center on Eq. (5), which, averaging over all lattice sites, gives

$$\langle \dot{s}(t) \rangle = (\kappa/2)[\langle s^2(t) \rangle - \langle q^2(t) \rangle] \tag{17}$$

Here, it is of interest to see if and how fast the ratio $\langle s^2(t) \rangle / \langle q^2(t) \rangle$ tends toward the value of 1. Furthermore, we check on the extent to which $s(\mathbf{x}, t)$ and $q(\mathbf{x}, t)$ are approximately Gaussian-distributed. A measure for this is how fast the ratios $\langle q^2(t) \rangle^{1/2} / \langle |q(t)| \rangle$ and $\langle s^2(t) \rangle^{1/2} / \langle s(t) \rangle$ reach the asymptotic value $(\pi/2)^{1/2}$.

One should note that for $\bar{d} > 4$, Eq. (16) would lead to a decay $t^{-\bar{d}/4}$ which is faster than t^{-1} . In this case we argue that $\langle q^2(t) \rangle$ can be neglected in Eq. (17) as compared to $\langle s^2(t) \rangle$; thus, assuming that $\langle s^2(t) \rangle^{1/2} \sim \langle s(t) \rangle$, it follows that $\langle s(t) \rangle$ obeys classical kinetics, i.e., $\langle s(t) \rangle \sim t^{-1}$. This imposes an upper marginal dimension of $d = 4$ and the corresponding limitation for the validity range of Eqs. (15) and (16). Furthermore, the ratio $\langle s^2(t) \rangle / \langle q^2(t) \rangle$ should diverge for $d > 4$.^(7,12) As a major consequence, we find that Eqs. (15) and (16) provide a lower bound to $A(t)$ for $\bar{d} < 4$.

We studied these points by solving numerically Eqs. (4) and (5). For the numerical treatment the ratio κ/τ^{-1} has to be fixed; for comparison to former approaches⁽¹¹⁾ we took κ as being equal to $2/\tau$.

In Fig. 1 various quantities are shown for $d = 1$. To clearly demonstrate the region of long-time behavior, the quantities were multiplied by their expected asymptotic forms, such that the asymptotic patterns appear as horizontal lines. A lattice of 4×10^5 sites was used. Plotted are $\langle |q(t)| \rangle t^{1/4} / (2C_1)$ and $\langle s(t) \rangle t^{1/4} / (2C_1)$. The displayed curves demonstrate that $\langle |q(t)| \rangle$ quickly reaches the asymptotic regime, whereas $\langle s(t) \rangle$ relaxes considerably more slowly. In the region of moderate times $\langle |q(t)| \rangle$ and $\langle s(t) \rangle$ differ significantly, and $\langle s(t) \rangle$, as presented in Fig. 1, shows a characteristic hump.

These patterns are compared with results taken from Monte Carlo (MC) calculations which were performed on Euclidean lattices and Sierpinski gaskets according to the following procedure: Initially equal numbers of A and B particles were placed randomly on the lattice and typically $10^6 - 10^7$ particles were used. Then a particle was picked randomly and was moved to a next neighbor position while simultaneously the time was incremented by the inverse of the number of particles still present in the sample. If one particle attempted to move onto a site occupied by a

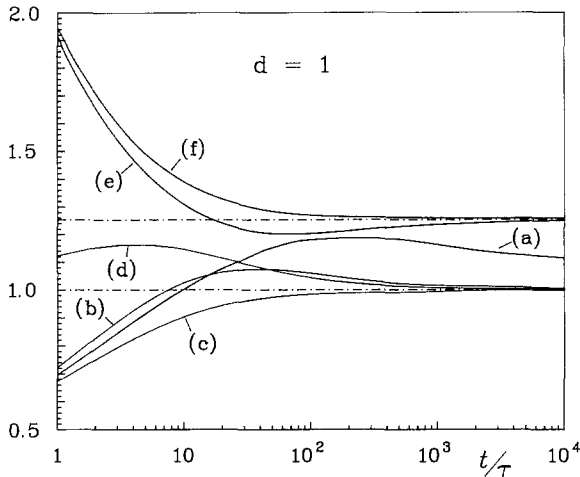


Fig. 1. Results from Monte Carlo (MC) simulations and from the deterministic approach for $d=1$. (a) MC result: $A_{MC}(t) t^{1/4}/C_1$. Deterministic result of the reaction-diffusion equations: (b) $\langle s(t) \rangle t^{1/4}/(2C_1)$, (c) $\langle |q(t)| \rangle t^{1/4}/(2C_1)$, (d) $\langle s^2(t) \rangle / \langle q^2(t) \rangle$, (e) $\langle s(t) \rangle / \langle s^2(t) \rangle^{1/2}$, (f) $\langle |q(t)| \rangle / \langle q^2(t) \rangle^{1/2}$. The dash-dotted lines indicate the values 1 and $(\pi/2)^{1/2}$. The initial concentration is $A_0 = B_0 = 0.05$.

particle of the opposite species, then both particles were removed from the lattice. The simulation results plotted as $A_{MC}(t) t^{1/4}/C_1$ [curve (a) in Fig. 1] show the same characteristic behavior as $\langle s(t) \rangle$ [curve (b)]; however, $A_{MC}(t)$ relaxes significantly more slowly to its asymptotic value than $\langle s(t) \rangle$. We view these differences between MC and deterministic data as resulting from the approximations introduced in the diffusion-reaction equations (1)–(3), which are thus limited in their ability to describe processes as complicated as particle annihilation. To complete the analysis, we display in Fig. 1 also the ratio $\langle s^2(t) \rangle / \langle q^2(t) \rangle$ [curve (d)], which shows a slow convergence to the value one. Finally, also plotted are the two ratios $\langle q^2(t) \rangle^{1/2} / \langle |q(t)| \rangle$ and $\langle s^2(t) \rangle^{1/2} / \langle s(t) \rangle$. Both ratios converge to the asymptotic value of $(\pi/2)^{1/2}$, which is consistent with q and s as being Gaussian-distributed at long times. Again the sum variable relaxes more slowly than the difference variable to its limiting value.

In Fig. 2 we present the same quantities as in Fig. 1 obtained for a 2D Sierpinski gasket. Equations (4) and (5) were solved on a gasket at the 11th iteration stage. The MC simulation was performed on a gasket at the 14th iteration stage. We remark the resemblance in the behavior of all quantities considered on the 2D Sierpinski gasket with those reported for the 1D lattice. Both the MC and the numerical method behave in similar fashion on regular lattices and on fractals; we conclude that the same limitations of the diffusion-equation method also applies to fractals.

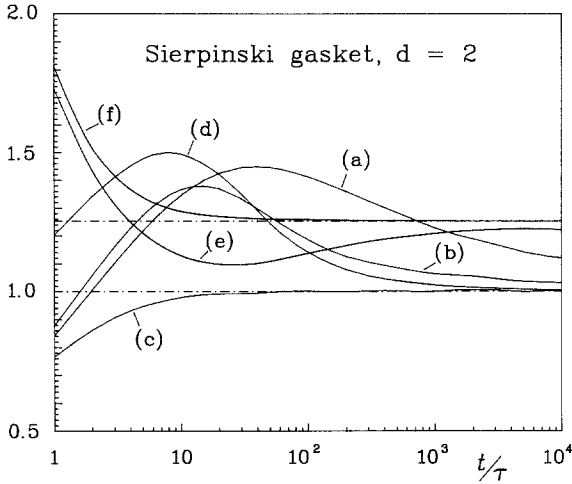


Fig. 2. As in Fig. 1, but for a 2D Sierpinski gasket. (a) From MC calculations $A_{MC}(t) t^{2/4}/C_0^2$; and from the solution of the reaction-diffusion equations: (b) $\langle s(t) \rangle t^{2/4}/(2C_0^2)$, (c) $\langle |q(t)| \rangle t^{2/4}/(2C_0^2)$, (d) $\langle s^2(t) \rangle / \langle q^2(t) \rangle$, (e) $\langle s(t) \rangle / \langle s^2(t) \rangle^{1/2}$, (f) $\langle |q(t)| \rangle / \langle q^2(t) \rangle^{1/2}$. The dash-dotted lines indicate the values 1 and $(\pi/2)^{1/2}$. The initial concentration is $A_0 = B_0 = 0.05$.

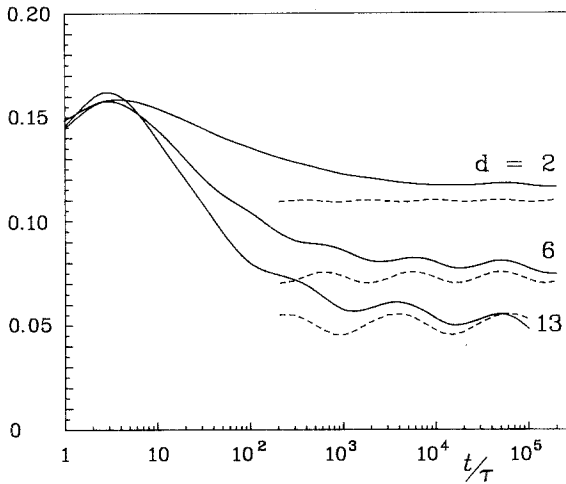


Fig. 3. Time evolution of the particle densities on Sierpinski gaskets. The MC simulations are displayed as $A(t) t^{d/4}$ and are given as full lines. The theoretical predictions $[A_0 P(0, 2t)/\pi]^{1/2} t^{d/4}$ are given by dashed lines. The embedding Euclidean dimension d is as indicated and the initial concentration was in all cases $A_0 = B_0 = 0.2$.

To emphasize this analysis further, we focus now on details typical for hierarchically-built structures. For these the autocorrelation function $P(0, t)$ shows an oscillatory behavior which is superimposed on the asymptotic power-law decay.^(17,18) The periods of these oscillations are related to the typical residence time of diffusing particles on hierarchical substructures and the oscillations amplitudes are larger for higher dimensions d . From Eq. (11) it is clear that $\langle q^2(t) \rangle$ should also follow the oscillatory behavior. Furthermore, the oscillations should also be visible in $A(t)$. This is in fact the case and is demonstrated in Fig. 3, where the decay is displayed for Sierpinski gaskets embedded in Euclidean lattices of dimensions $d=2, 6$, and 13 . In order to highlight the oscillatory behavior, the simulation results are plotted as $A_{MC}(t) t^{d/4}$. They are compared with Eq. (15), $[A_0 P(0, 2t)/\pi]^{1/2} t^{d/4}$, where $P(0, t)$ was obtained from independent numerical calculations.⁽¹⁸⁾

For a Sierpinski gasket in $d=2$ the oscillations are hardly detectable and the MC calculation tends smoothly to the $P(0, t)$ -type expression; however, the relaxation to the asymptotic behavior occurs at times $t/\tau \gtrsim 10^4$. For Sierpinski gaskets in ($d=6$)- and ($d=13$)-dimensional spaces the oscillations are clearly visible: also the periods and the phases are in qualitative agreement with the $P(0, t)$ -type forms. For $d=2$ and $d=6$, the deviations between simulation and $P(0, t)$ evaluation are of the order of 5–10% at long times. For $d=13$ the oscillatory behavior is again very well reproduced; on the other hand, care has to be used for t values larger than $t/\tau > 10^4$, where finite-size effects begin to be felt.

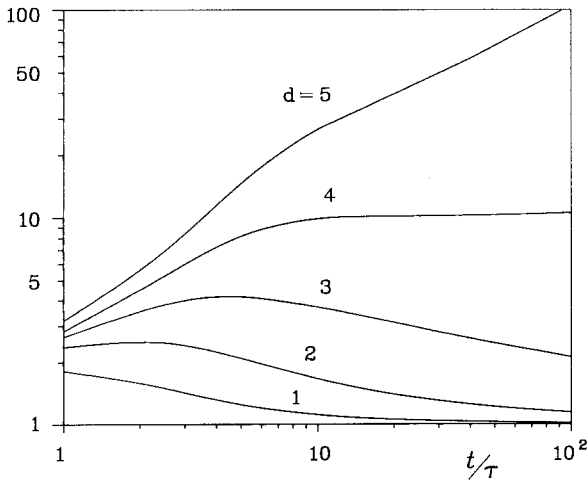


Fig. 4. The ratio $\langle s^2(t) \rangle / \langle q^2(t) \rangle$. Results are plotted for hypercubic lattices of dimensions $d=1-5$.

In Fig. 4 we present the ratio $\langle s^2(t) \rangle / \langle q^2(t) \rangle$ calculated for regular lattices for dimensions $d=1$ and $d=5$. Lattice sizes of some 10^6 sites were used to solve Eqs. (4) and (5). For $d=2$ the convergence to the limiting value of 1 is still visible, although slower than in $d=1$; for $d=3$ the convergence is even slower. The marginal behavior for $d=4$ is evident: $\langle s^2(t) \rangle / \langle q^2(t) \rangle$ reaches a plateau for $t/\tau \simeq 10$; furthermore, in $d=5$, $\langle s^2(t) \rangle / \langle q^2(t) \rangle$ increases steadily with time. We infer that approximating $A(t)$ through $q(t)$ is justified only in low-dimensional spaces.

Concluding, our analysis has shown that for low-dimensional lattices the deterministic approach based on reaction-diffusion equations provides a reasonable description of the reaction process. In fact, expression (15) represents a lower bound for the density decay, so that Eq. (16) follows: $A(t) \sim t^{-\alpha}$ with $\alpha = \min(\tilde{d}/4, 1)$. The numerical results obtained from both the deterministic and the stochastic approaches support these findings.

ACKNOWLEDGMENTS

A grant of computer time from the Rechenzentrum der ETH-Zürich and the support of the Deutsche Forschungsgemeinschaft (SFB 213) and of the Fonds der Chemischen Industrie are gratefully acknowledged.

REFERENCES

1. A. A. Ovchinnikov and Y. B. Zeldovich, *Chem. Phys.* **28**:215 (1978).
2. D. Toussaint and F. Wilczek, *J. Chem. Phys.* **78**:2642 (1983).
3. P. Meakin and H. E. Stanley, *J. Phys. A* **17**:L173 (1984).
4. K. Kang and S. Redner, *Phys. Rev. Lett.* **52**:955 (1984).
5. G. Zumofen, A. Blumen, and J. Klafter, *J. Chem. Phys.* **82**:3198 (1985).
6. A. Blumen, J. Klafter, and G. Zumofen, in *Optical Spectroscopy of Glasses*, I. Zschokke, eds. (Reidel, Dordrecht, 1986), p. 199.
7. S. Havlin and D. Ben-Avraham, *Adv. Phys.* **36**:695 (1987).
8. M. Bramson and J. L. Lebowitz, *Phys. Rev. Lett.* **61**:2397 (1988); **62**:694 (1989).
9. Wen-Shyan Sheu, K. Lindenberg, and R. Kopelman, *Phys. Rev. A* **42**:2279 (1990).
10. H. Schnörer, V. Kuzovkov, and A. Blumen, *Phys. Rev. Lett.* **63**:805 (1989).
11. E. Clément, L. M. Sander, and R. Kopelman, *Phys. Rev. A* **39**:6455 (1989).
12. B. J. West, R. Kopelman, and K. Lindenberg, *J. Stat. Phys.* **54**:1429 (1989).
13. I. M. Sokolov and A. Blumen, *Phys. Rev. A* **43**:2714 (1991).
14. Zhang Yi-Cheng, *Phys. Rev. Lett.* **59**:1726 (1987).
15. G. Zumofen, J. Klafter, and A. Blumen, *Phys. Rev. A* **43**:7068 (1991).
16. K. Lindenberg, Wen-Shyan Sheu, and R. Kopelman, *Phys. Rev. A* **43**:7070 (1991).
17. B. O'Shaughnessy and I. Procaccia, *Phys. Rev. A* **32**:3073 (1985).
18. J. Klafter, G. Zumofen, and A. Blumen, *J. Phys. A*, in press.